Remote Sensing of Environment 233 (2019) 111403

Contents lists available at ScienceDirect

Remote Sensing of Environment

journal homepage: www.elsevier.com/locate/rse

# Prevalence of multiple forest disturbances and impact on vegetation regrowth from interannual Landsat time series (1985–2015)

Txomin Hermosilla[a,*], Michael A. Wulder[a], Joanne C. White[a], Nicholas C. Coops[b]

[a] Canadian Forest Service (Pacific Forestry Centre), Natural Resources Canada, 506 West Burnside Road, Victoria, British Columbia V8Z 1M5, Canada
[b] Integrated Remote Sensing Studio, Department of Forest Resources Management, University of British Columbia, 2424 Main Mall, Vancouver, BC V6T 1Z4, Canada

ARTICLE INFO

Edited by Emilio Chuvieco

*Keywords:*
Canada
Change detection
Fire
Harvest
Recovery
Overlapping disturbances
National

ABSTRACT

Given long time series of satellite imagery, multiple disturbances can be detected for a particular location at different points in time. We assessed multiple disturbances for the 650 Mha of Canada's forested ecosystems using annual change information derived from Landsat time series imagery (1985–2015). Changes were typed by agent (fire, harvest, and non-stand replacing). Spectral change rate and time between successive disturbances were used to characterize disturbance-type combination differences. Short-term spectral recovery following the last disturbance was compared to a reference sample of pixels disturbed only once. Results indicated that of the 97.6 Mha disturbed, 13.5 Mha have had two or more disturbances, with low magnitude non-stand replacing disturbances involved in the majority of occurrences (77.2%). The total area disturbed represents 18.27% of forest ecosystems, with 2.53% having multiple disturbances and 0.54% having multiple stand-replacing disturbances. Systematic time series-based investigation of multiple disturbance events and agents provides insights on forest disturbance dynamics and recovery processes.

## 1. Introduction

Forest ecosystems are constantly undergoing alteration by both natural and anthropogenic drivers, and information regarding the location and nature of these changes is required for scientific, policy, and fulfilling management and reporting needs (Goward et al., 2008; Kangas and Maltamo, 2006). The capture of forest disturbances is important to inform forest inventories to ensure an accurate and up-to-date portrayal of forests (Gillis and Leckie, 1996). Forest disturbances modulate the carbon flux between the biosphere and the atmosphere, therefore detailed knowledge of disturbances over time and space is critical to predict present and future carbon dynamics (Hirsch et al., 2004; Kurz et al., 2009). As such, carbon accounting programs require information on forest change related aspects including pre- and post-disturbance cover, disturbance agent, and magnitude of disturbance (Wulder et al., 2004). These programs are designed to monitor and report on forest carbon stocks and stock changes and are commonly informed by forest inventories as a core data source (Kennedy et al., 2018; Kurz et al., 2008; Wilson et al., 2013).

Along with climatic and topographic factors, forest disturbance, regeneration and recovery characteristics are also influenced by disturbance history (Kulakowski and Veblen, 2002). Dynamic forested ecosystems present complex interactions among multiple disturbance types which overlap through time over a range of severities (Oliver and Larson, 1990). Following major disturbances there can be a change in the species composition that in turn can modify forest structure and productivity altering a locations' predisposition to subsequent disturbances (Bigler et al., 2005; Lavoie and Sirois, 1998). Interactions between multiple disturbances are defined as *linked* when the occurrence or severity of the first event has legacies that affect that of the second disturbance (Edwards et al., 2015), or *compounded* when the likelihood or speed of recovery (to a similar state and function) from the subsequent disturbance is altered (Buma, 2015). In a changing climate scenario where disturbance events may increase in both their frequency and severity, the analysis of multiple disturbance interactions is important since they have the potential to exceed the ecological resilience of an ecosystem, implying potential non-recovery or an ecosystem shift (Beisner et al., 2003; Buma and Wessman, 2011; Turner et al., 2019). These interactions, however, have rarely been quantitatively examined since modeling requires temporally-comparable and spatially-explicit datasets, which historically have not been available (Bebi et al., 2003).

Remote sensing technology is ideally suited to enable monitoring systems that capture timely information describing forest condition and dynamics over large areas and long time periods (Banskota et al., 2014; Wulder et al., 2004). Free and open access to the United States Geological Survey (USGS) Landsat image archive (Woodcock et al., 2008)

* Corresponding author.
*E-mail address:* txomin.hermosilla@canada.ca (T. Hermosilla).

https://doi.org/10.1016/j.rse.2019.111403
Received 14 May 2019; Received in revised form 7 August 2019; Accepted 26 August 2019

provides users with high-quality analysis-ready data at informative spatial and temporal resolutions for analyzing natural and human-induced changes in terrestrial ecosystems (Wulder et al., 2012). A direct consequence of this modification to data accessibility policy is the emergence of novel techniques to monitor forested ecosystems (Wulder et al., 2019; Zhu et al., 2019). Methods for seamlessly assembling image data into composites representing large areas in a systematic and consistent fashion have been developed (Griffiths et al., 2013; Hermosilla et al., 2015a; Roy et al., 2010; White et al., 2014). Similarly, the richness and multi-decadal depth of Landsat image archive (Wulder et al., 2016) has fostered the development of change detection approaches based on the analysis of dense time series of imagery (Hermosilla et al., 2015b; Huang et al., 2010; Kennedy et al., 2010; Verbesselt et al., 2010; Zhu and Woodcock, 2014). These change detection approaches are typically based on the temporal analysis of spectral trajectories and enable both stand replacing (i.e., discrete changes such as wildfire and harvest) and non-stand replacing disturbances (more subtle or longer term events such as defoliation, water stress, etc.) to be discriminated with high sensitivity and reliability (Kennedy et al., 2014). Furthermore, these change detection approaches effectively integrate time series of imagery acquired with Landsat-4 and -5 Thematic Mapper (TM), −7 Enhanced Thematic Mapper Plus (ETM+), and -8 Operational Land Imager (OLI), which has resulted in more than three decades of continuous observations at 30-m spatial resolution. Common to spectral-trajectory-based change detection approaches is the capacity to independently detect and characterize several disturbances occurring over the same geographic space (pixel) but at different times over the analyzed period. While multiple disturbances are captured in the time series, these events are not commonly spatially represented or reported upon. Given the temporal depth of Landsat measures (from 1972 at 60-m and since 1982 at 30-m spatial resolution), multiple disturbances at a particular location are increasingly likely.

With increasing disturbance frequencies expected as a result of changing climatic conditions (Price et al., 2013), there is likewise an increase in the likelihood of multiple disturbances occurring in rapid succession relative to vegetation recovery rate (Bradford et al., 2012). The detailed information provided by a time series of Landsat imagery captures and describes forest disturbances and subsequent vegetation regrowth for several decades (Kennedy et al., 2010; White et al., 2017), which can assist in improving our understanding on the behaviour and consequences of multiple, interacting disturbances. The aim of this research is an improved understanding of the frequency and nature of multiple disturbance dynamics for Canada's forested ecosystems. Using Landsat time series imagery and derived forest change products, we analyzed the frequency, distribution and agents of multiple forest disturbances, and related short-term vegetation recovery, for the period 1985–2015. Systematic analysis of multiple disturbances using dense time series of remotely sensed imagery informs on both forest disturbance dynamics and recovery processes. Results of this research can inform projections of forest regrowth following multiple disturbance events in complex-change forest environments and are valuable to sustainable forest management and carbon accounting information needs.

## 2. Study area

Canada's forested ecosystems constitute ~650 Mha (534.3 Mha of net forested area excluding land surface water; White et al., 2017), or 65% of Canada's total area (Wulder et al., 2008). These forested ecosystems cover a broad range of ecological and climatic conditions, and are highly variable in their abundance of treed areas, productivity and growing conditions, as well as the degree of forest management and human population density. Remote northern forests are generally unmanaged, with little to no fire suppression or harvesting tenure arrangements. Forest inventory data in these areas are therefore also limited. In contrast, southern latitudes of Canada's forested ecosystems are subject to forest management practices such as harvest tenure agreements, inventory generation, and other sustainable forest management initiatives. Although fire suppression activities are more common in these managed forest, wildfires are still an annual occurrence. Fire is the main stand replacing disturbance in Canada's forests (Fig. 1) (Boulanger et al., 2012). The annual average area disturbed by wildfire is approximately 1.56 Mha, compared to the 0.65 Mha disturbed by harvest (White et al., 2017). Insects impact an estimated 16.6 Mha on average each year with varying defoliation or mortality effects.[1] The influence of multiple disturbances on Canada's forests has been highlighted by various studies that have examined disturbance interactions and impacts (Cobb et al., 2007; Maynard et al., 2014; Pidgen and Mallik, 2013; Vepakomma et al., 2010; Woods et al., 2017).

## 3. Methods

### 3.1. Landsat time series data and derived forest change information

Forest change information was produced using the Composite2Change or C2C approach (Hermosilla et al., 2016). This methodology computes annual best-available pixel (BAP) image composites by selecting optimal pixel observations from all available archived Landsat-5 TM, -7 ETM+, and −8 OLI imagery (Hermosilla et al., 2017) from 1984 to 2016 over the 1280 scenes (path/row) covering Canada (White and Wulder, 2014). This analysis utilized Landsat images from USGS Collection-2 with surface reflectance values generated using LEDAPS (Masek et al., 2006; Schmidt et al., 2013). Cloud and cloud shadow information was derived using the Fmask algorithm (Zhu and Woodcock, 2012).

All pixels were ranked using a set of compositing scoring functions to identify optimal observations (Hermosilla et al., 2016; White et al., 2014). Scoring functions included proximity to target date (August 1st, Julian day 213 ± 30 days), occurrence and distance to clouds and their shadows, haze opacity, and acquisition sensor (i.e., lower rank for Landsat-7 ETM+ following the scan line corrector failure). With the inclusion of Landsat-8 OLI data in C2C from 2013 forward, the haze opacity score was no longer used. On average, 14.2% of pixels are identified as having data gaps each year (Hermosilla et al., 2016). The annual BAP composites are then further processed to remove any residual cloud, shadow, and haze. Noise is distinguished from real change using an approach that compares anomalous values (i.e., spikes) in the pixel series with the difference between the pixel in the preceding and subsequent year. If the spike is larger than a pre-determined threshold (determined using a sensitivity analysis) times the difference, the pixel is flagged as noise (Kennedy et al., 2010). This detection of anomalous values is applied independently to each of the six Landsat bands. If a pixel is flagged as noise in three or more of the six spectral bands, then the pixel is labelled no data. As a result additional data gaps (~8.4% on average annually; Hermosilla et al., 2016) are added to the annual BAP composites. To facilitate trend detection, a preliminary infilling of data gaps is undertaken over temporal series of Normalized Burn Ratio (NBR) values (Key and Benson, 2006). The NBR index incorporates the short-wave infrared wavelength and is understood to inform on forest structure (Cohen and Goward, 2004; Horler and Ahern, 1986). NBR suitability and performance for forest change detection is supported by previous research (Cohen et al., 2018; Hermosilla et al., 2016; Pickell et al., 2016). Temporal trends and changes are identified with linear segments describing spectral trajectories and remove noise using a bottom-up breakpoint selection algorithm (Keogh et al., 2001). This algorithm divides temporal series with n elements (number of years) into n-1 segments. Potential segments are evaluated by calculating the vertical differences between the best-fit line for the segment and the NBR values, and then squaring and summing them (i.e., the Root Mean

[1] http://nfdp.ccfm.org/en/index.php

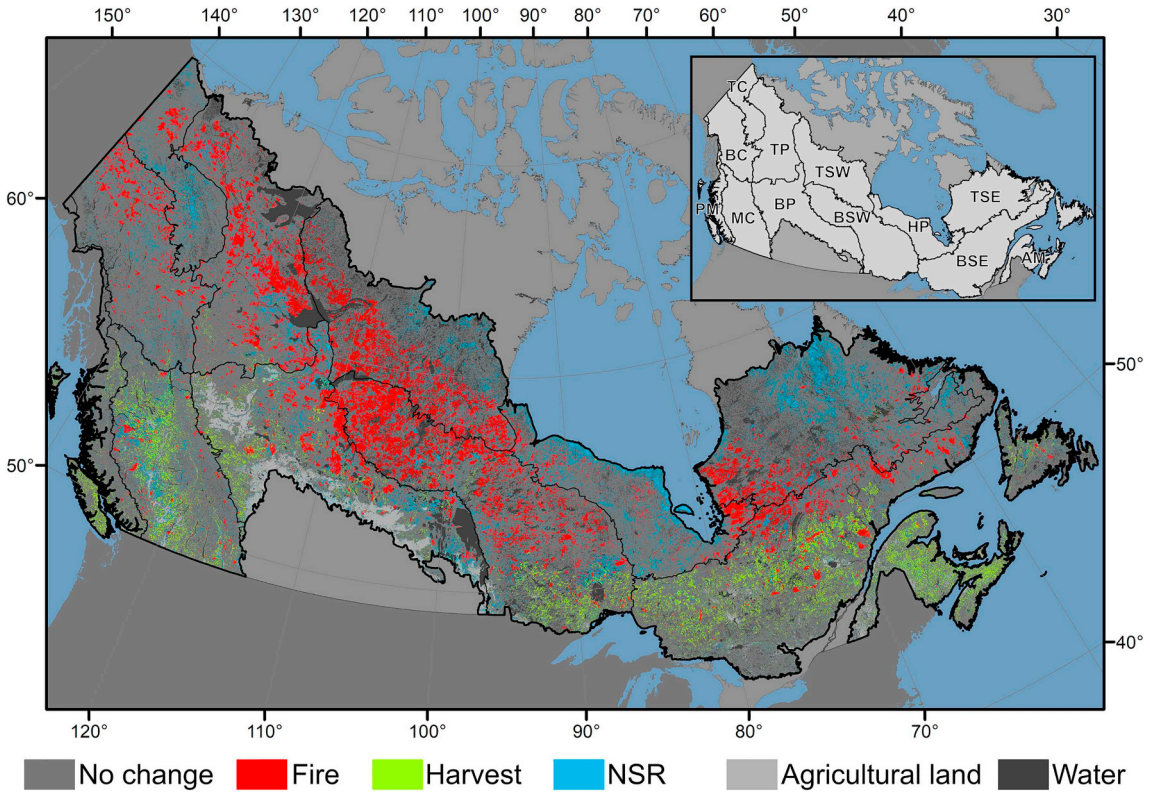


**Fig. 1.** Area disturbed by fire, harvest, and non-stand replacing (NSR) disturbances for the period 1985–2015, as identified using the Composite2Change (C2C) approach (Hermosilla et al., 2016). Map shows the greatest disturbance based on disturbance magnitude. Legend only applicable within Canada's forested ecosystems. Inset map displays Canada's forested ecozones: Atlantic Maritime (AM), Boreal Cordillera (BC), Boreal Plains (BP), Boreal Shield East (BSE), Boreal Shield West (BSW), Hudson Plains (HP), Montane Cordillera (MC), Pacific Maritime (PM), Taiga Cordillera (TC), Taiga Plains (TP), Taiga Shield East (TSE), and Taiga Shield West (TSW). Agricultural land provided by Agriculture and Agri-Foods Canada. Water bodies derived from Hermosilla et al. (2018).

Square Error, RMSE). The RMSE is then used to evaluate the cost of merging each pair of adjacent segments, resulting in the pair with the lowest cost being merged. The cost value is then recomputed and the process iterated until reaching the maximum merging cost (0.125) or the maximum number of segments (i.e., six; Hermosilla et al., 2017). Temporal trends with negative slopes represent disturbances in vegetation and are identified as changes. Changes are detected between 1985 and 2015 (i.e., no change events are detected the first and last years of the time-series: 1984, 2016). Temporal trends and changes in each pixel series are then used to assign synthetic or proxy values to the data gaps generated from the aforementioned noise detection process. The output of this process are annual gap-free surface reflectance composites with temporally fitted spectral values, forest changes, and a suite of metrics characterizing the forest changes (Hermosilla et al., 2015a).

Changes detected in the time series were then allotted to disturbance agent classes using an object-based image approach, the change hierarchy introduced in Hermosilla et al. (2015b), and a Random Forests model. At the highest level, pixels are partitioned as change and no change. Based on their characteristics (spectral, temporal and geometrical), changed pixels are separated into stand and non-stand replacing classes. Stand replacing changes are abrupt disturbances that generally involve a major removal of vegetation (e.g., wildfire, harvest). Non-stand replacing disturbances are gradual changes in the vegetation status and health that do not necessarily require a change in land cover class (i.e., disease, insects, water stress, and decline). Due to its spatial resolution, Landsat imagery is suboptimal for mapping and detecting roads (Stewart et al., 2009) and road construction changes (Hermosilla et al., 2016), especially in forest environments where roads can be temporary, narrow, sub-pixel, as well as having variable reflectance characteristics due to the road surface present (e.g., dirt, gravel, or paved). Therefore, and as a result of the lower reliability on the attribution of roads, these changes were excluded from further analysis. As the focus of this research is forested ecosystems, changes in agricultural lands were identified and excluded from further analysis using a mask provided by Agriculture and Agri-Foods Canada. C2C forest change products were independently assessed following the approach outlined in Olofsson et al. (2014) resulting in an overall accuracy of 89% for the change detection and 92% for the change classification to a change type. The change year was correctly identified in 89% of cases, with 98% of cases detected within ± 1 year. For complete and detailed accuracy assessment results, please see Hermosilla et al. (2016).

### 3.2. Analysis of multiple disturbances

We analyzed the Landsat-derived forest change layers to map and summarize disturbances in Canada's net forested ecosystem area (which excludes land surface water and includes agricultural lands, as per White et al., 2017) between 1985 and 2015, reporting on pixels that underwent multiple disturbances ($n$ = 150,127,388 pixels). We further analyzed those pixels that had two disturbances during the analysis period ($n$ = 141,335,955 pixels) according to their disturbance agent (i.e., fire, harvest, and non-stand replacing disturbance), and time elapsed between the two disturbance events. The distribution of metrics spectrally characterizing the change and the post-disturbance vegetation recovery of these pixels were studied based on the order of occurrence (first or second). Instances with three or more disturbances were not analyzed further due to the small area impacted (0.81% of the total disturbed area). To define a baseline scenario that enabled comparing the effect of multiple disturbances on change rate and recovery, we first derived a random sample from pixels that had one single

disturbance event during the analyzed period. These pixels provided reference values that were then compared to pixels with two detectable disturbances.

Disturbances were spectrally characterized using the C2C change rate metric, which is computed as the ratio of change magnitude and change persistence (Hermosilla et al., 2016):

$$rate_d = \frac{\Delta NBR_d}{p} \quad (1)$$

where $p$ is the persistence or duration of the change segment, and $\Delta NBR_d$ is the change magnitude:

$$\Delta NBR_d = NBR_{y-p} - NBR_y \quad (2)$$

where $NBR_y$ is the NBR value at the beginning of the disturbance segment, and $NBR_{y-p}$ is the NBR value at the end of the disturbance segment.

Post-disturbance vegetation recovery was characterized using the recovery indicator metric (Kennedy et al., 2012; White et al., 2017). The recovery indicator is a relative measure of spectral vegetation recovery which is conditioned by the change magnitude:

$$RI = \frac{\Delta NBR_{regrowth}}{\Delta NBR_d} \quad (3)$$

where $\Delta NBR_{regrowth}$ indicates the absolute change in NBR at five years following the disturbance (Eq. 4).

$$\Delta NBR_{regrowth} = NBR_{y5} - NBR_y \quad (4)$$

where $NBR_{y5}$ is the NBR value at 5 years post-disturbance and $NBR_y$ is the NBR value in the year of disturbance. Accounting for the need to have a 5-year post-disturbance period, we considered only those pixels disturbed between 1985 and 2011 to compute the recovery indicator metric.

Fig. 2 shows examples of spectral NBR time series with two disturbances. The time series in Fig. 2A exemplifies a scenario comprised of six spectral trends (segments AB, BC, CD, DE, EF, FG) from which two segments have negative slopes and represent disturbances (segments BC and EF). The first disturbance starts in $y_B$, finishes in $y_C$, and has a persistence of one year ($y_C$-$y_B$). The second disturbance starts in $y_E$, finishes in $y_F$, and has a persistence of seven years ($y_F$-$y_E$). Time between these two disturbances is computed as the number of years between the end of BC ($y_C$) and the beginning of EF ($y_E$), and is 11 years in this particular example. The change rate for the first disturbance is computed as the ratio between the change magnitude $\Delta NBR_{dBC}$ divided by the change persistence ($y_C$-$y_B$). Similarly, the change rate for the second disturbance is computed as the ratio between the change magnitude ($\Delta NBR_{dBC}$) divided by the disturbance persistence ($y_F$-$y_E$). The recovery indicator for the second disturbance is computed as the ratio between the $\Delta NBR_{regrowth}$ ($\Delta NBR_{regrowthF+5}$) at five years following the disturbance ($y_{F+5}$) divided by the change magnitude ($\Delta NBR_{dEF}$). The recovery indicator can be computed for any disturbance. As the aim of this analysis is to test compounded interaction of multiple disturbances (i.e., variations in the likelihood or speed of recovery from the secondary disturbance; Buma, 2015), we only calculated recovery indicator for the second disturbance. The time series shown in Fig. 2B is made of three spectral trends (segments AB, BC, CD) from which segment AB and BC represent disturbances. The first disturbance (segment AB) is an example of non-stand replacing disturbance that starts in $y_A$, finishes in $y_B$, and has a persistence of 18 years ($y_B$-$y_A$). Non-stand replacing disturbances are by definition low magnitude and typically persist for several years. The second disturbance (segment BC) starts in $y_B$ and finishes in $y_C$, having a persistence of one year ($y_C$-$y_B$), and represents a stand replacing disturbance (i.e., fire, harvest). Whereas non-stand replacing disturbance year is the culmination of a multi-year process; wildfire and harvest events are labelled with the actual year of disturbance. In this case, the time between disturbances is zero, since it the ending year of the first disturbance segment AB ($y_B$) corresponds with the start year of the second disturbance segment BC ($y_B$).

## 4. Results

The spatial distribution of the number of disturbance events in Canada's forested ecosystems is mapped in Fig. 3, with insets over selected areas to relate local detail within especially dynamic and complex environments shown (by ecozone), Montane Cordillera (Fig. 3A), Boreal Shield West (Fig. 3B), Hudson Plains (Fig. 3C), and Boreal Shield East (Fig. 3D).

Table 1 shows the summary of disturbed forest area with reference to the number of disturbances present between 1985 and 2015. During this 30-year time period, approximately 18.27% of Canada's net forested ecosystem area (exclusive of water) was impacted by wildfire, harvest, and non-stand replacing disturbances. On an annual basis the average, area disturbed by wildfire is 1.61 Mha and harvest is 0.64 Mha. These results indicate a 3% increase in the average annual area disturbed by wildfire and a 2% decrease in area disturbed by harvest when considering the period 1985–2015 relative to the annual rates reported by White et al. (2017) for the 1985–2010 period. The majority of the disturbed forest area (86.16%) had only a single disturbance over the analyzed period, while 13.03% of the disturbed area had two disturbance events, representing approximately 2.38% of Canada's net forested ecosystem area (excluding water). Further, 0.81% of the forest disturbance area had three or more disturbance events (i.e., 0.15% of Canada's net forest area).

The distribution of disturbances related to their change type at disturbance order (first or second disturbance event) is shown with a Sankey diagram in Fig. 4. Sankey diagrams represent cross-tabulated data graphically using flows connecting nodes in a network (Schmidt, 2008). These diagrams are well suited to present information on land cover dynamics and change over multiple times, since they enable emphasizing the size and direction of these flows within a system (Cuba, 2015).

Our results indicated that non-stand replacing (low magnitude or longer term events) disturbances were involved in the majority of the multiple disturbance occurrences, with 77.2% of these cases involving non-stand replacing as first and/or second change type. The largest proportion of multiple disturbances (33.6%) were related to consecutive non-stand replacing disturbances. Non-stand replacing disturbances followed by fire represented 26.3%, and non-stand replacing followed by harvest events were 7% of the two multiple disturbance area. Small portions of area initially affected by fire were later harvested (1.1%), while the opposing situation (i.e., harvesting followed by wildfires) was slightly more common (2.3%). Of the areas that had two disturbances in the analysis period, 11% were affected by two consecutive wildfires, and 8.5% by two consecutive harvest events.

Histograms of years elapsed between the first and second disturbance for each combination of change types are shown in Fig. 5 (note that y-axis ranges are different for each histogram). The occurrence of a second fire following another wildfire had the greatest spread in years elapsed, with two maxima located at 16 and 23 years after the first disturbance. Similarly, the harvest-fire interaction of disturbances also resulted in a wide distribution of years elapsed. Values, however, are skewed towards the earlier years following the first disturbance. Both fire-harvest and harvest-harvest interactions were notably skewed towards the earlier years. Non-stand replacing disturbances followed by fire and non-stand replacing followed by harvest had major histogram maxima right after the first disturbance event (time since disturbance = 0; see example in Fig. 2B). The occurrence of two successive non-stand replacing disturbances shows a clear maxima a year after the first disturbance. The distribution of the histogram values for fire followed by non-stand replacing spanned out across the earlier years following the event. Non-stand replacing following harvest mostly occurred immediately after the first disturbance.

The distribution of change rate values by change type is shown in

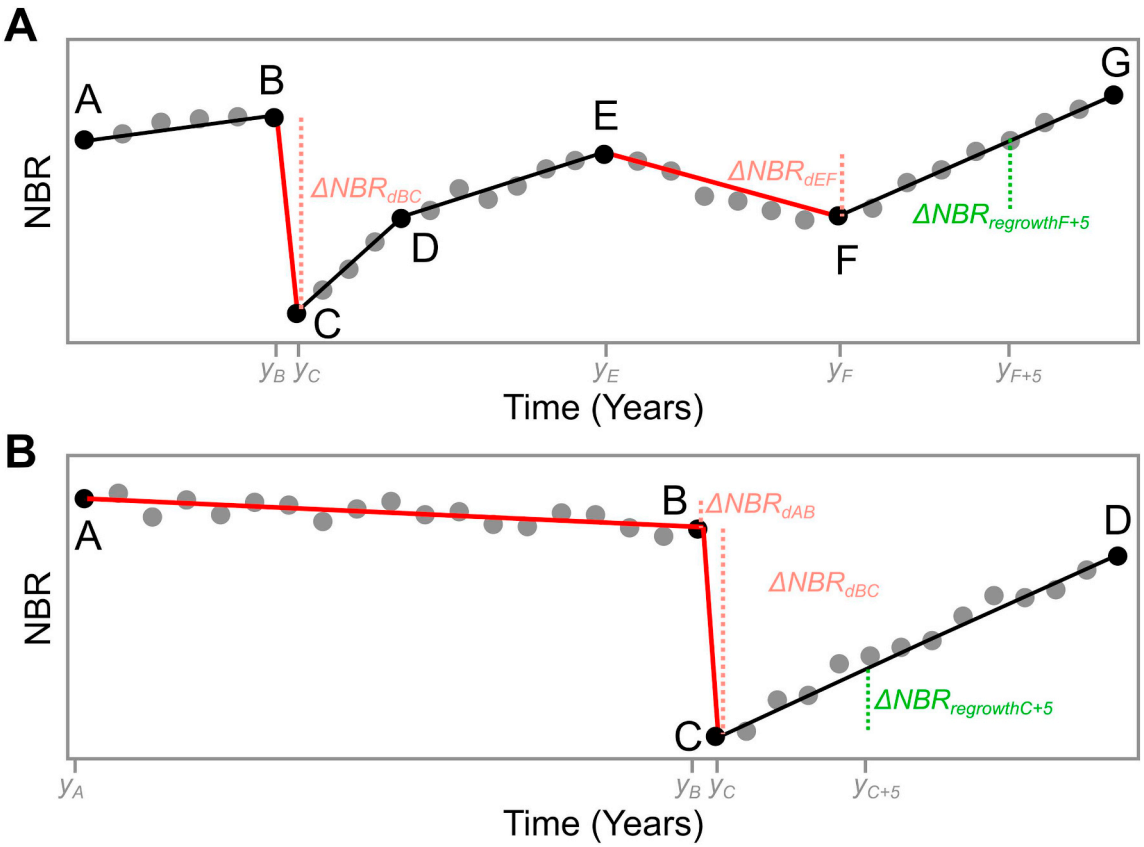


**Fig. 2.** Example of spectral trends and breakpoints used to identify disturbance segments (shown in red) and compute change metrics for a single pixel of Landsat time series data. (A) $\Delta NBR_{dBC}$ and $\Delta NBR_{dEF}$ represent the disturbance magnitude for the disturbances BC and EF, respectively. $\Delta NBR_{regrowthF+5}$ represents the post-disturbance regrowth five years following the EF disturbance. (B) $\Delta NBR_{dAB}$ and $\Delta NBR_{dBC}$ represent the disturbance magnitude for the disturbances AB and BC, respectively. $\Delta NBR_{regrowthC+5}$ represents the post-disturbance regrowth five years following the BC disturbance. (For interpretation of the references to color in this figure legend, the reader is referred to the web version of this article.)

Fig. 6. For reference, Fig. 6A shows the change rate from pixels where one single disturbance was given during the analysis period. Wildfires had the highest annual change rate values (median = 0.59), followed by harvest (median = 0.41) and non-stand replacing disturbances present the lowest values (median = 0.15). Fig. 6B shows the distribution of change rate values for first and second change for each pair of change type combination. Fires presented similar distribution of change rate values with independence of the position of this event (first or second disturbance) or the accompanying change type (fire, harvest, or non-stand replacing). Similarly, first harvest events showed comparable values to the reference ones. Second harvest events, however, had lower change rate when following fire (median = 0.24) or previous harvest disturbances (median = 0.29). Non-stand replacing disturbances followed by fire and harvest events resulted in the lowest change rate values (medians = 0.02 and 0.04, respectively). However, the dispersion of non-stand replacing change rate values when followed by harvest (interquartile range, IQR = 0.10) is markedly greater than when followed by fire (IQR = 0.05).

Fig. 7 shows the distribution of the recovery indicator metric following single disturbance events (as control), compared to the distribution for multiple disturbances. Note that although there are differences in the median values, there is also greater variation in the distribution of the recovery indicator metric, suggesting that multiple disturbances increase variability in spectral recovery. The recovery indicator metric values when fire is the second event (Fig. 7A) have a similar distribution than single wildfire disturbances (median = 0.33) with the exception of harvest-fire interaction which resulted in larger recovery indicator values (0.41). Compared to single harvest events (median = 0.56; Fig. 7B), the recovery indicator metric for the harvest-harvest interaction reached slightly higher values (median = 0.62). In contrast, harvest after fire disturbances resulted in lower recovery indicator metric values (median = 0.34). Single non-stand replacing disturbances are characterized to present the larger variability (range = −0.55–1.75) and large values (median = 0.59) on the resulting recovery indicator metric, similarly to harvest followed by non-stand replacing disturbances and two consecutive non-stand replacing disturbances (Fig. 7C). The fire followed by non-stand replacing disturbances, however, displays a markedly smaller variability (range = −0.25–0.89) and lower recovery indicator metric values (median = 0.30).

## 5. Discussion

In this research, we mapped, reported, and analyzed areas that presented multiple disturbances across Canada's forested ecosystems, with reference to their disturbance agent, the time elapsed between these disturbances, and the spectral characterization of both the disturbance event itself and the post-disturbance vegetation regrowth. This multifaceted analysis was enabled by the Landsat-derived datasets produced using the Composite2Change (C2C) approach which included annual Canada-wide seamless surface reflectance composites and land change information products that characterize and categorize forest disturbances by disturbance agent (Hermosilla et al., 2016) as well as a quantification of vegetation return following disturbances (White et al., 2017). Akin to other widely used change detection approaches (Zhu, 2017) based on the temporal analysis of pixels using dense time series of Landsat imagery (Huang et al., 2010; Kennedy et al., 2010; Verbesselt et al., 2010; Zhu and Woodcock, 2014), C2C enables the

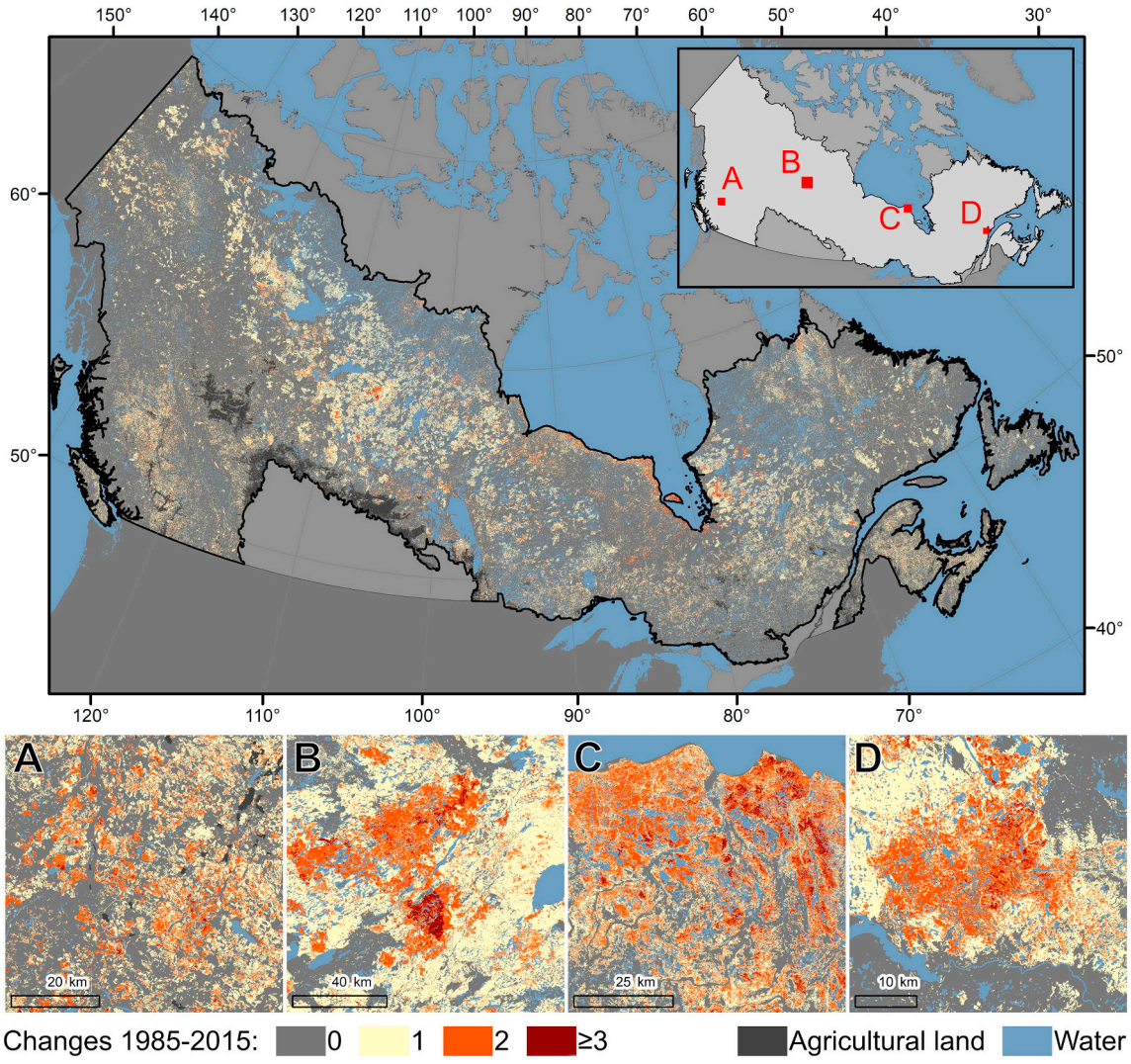


**Fig. 3.** Spatial distribution of the number of disturbances detected in Canada's forested ecosystems between 1985 and 2015. Regional spatially detailed insets showing multiple disturbances in (A) Montane Cordillera, (B) Boreal Shield West, (C) Hudson Plains, and (D) Boreal Shield East.

detection and characterization of multiple disturbances occurring in the same pixel at different times within the analyzed period. While computed, multiple disturbance information, however, is not commonly assessed (Thomas et al., 2011) and is often subsumed in the graphical representation and statistical reporting of the changes in favour of simplifications representing the greatest or latest disturbance recorded during the analysis period. Adding additional years to a given existing time series offers opportunities to confirm or observe alterations to previously reported trends. When compared to White et al. (2017) relating disturbance trends from 1985 to 2010, the results of the current analysis (1985 to 2015) with an additional five years of data show a 2% decrease in the average annual area disturbed by harvesting and a 3% increase in the annual area disturbed by fires. It is also possible that more notable regional changes to existing trends can be muted in national statistics. Previous research (Coops et al., 2018) only found evidence of regionally significant increasing trends of burned area in specific ecozones, namely the Montane Cordillera, Taiga Plains, and Taiga Shield West. Increasing disturbance rates would certainly impact the interpretation of results on multiple disturbance interactions and post-disturbance vegetation regrowth, and suggest a need for epochal analyses (e.g., Frazier et al., 2015) of both multiple disturbance interactions and vegetation regrowth.

Studying the multiple disturbance interactions is of value as multiple disturbances can result in broad changes to the composition and configuration of affected forest stands. Short-time intervals between disturbances may not have afforded opportunity for the forest to recover from the initial disturbance, and this can result in regional legacies of modified ecosystem structure into the future (Edwards et al., 2015; Pidgen and Mallik, 2013). Climate change scenarios typically anticipate an increase in the severity and frequency of natural disturbances (Price et al., 2013). Consequently, as disturbance frequencies increase, the possibility of multiple forest disturbances occurring before the recovery of previous events becomes increasingly likely (Bradford et al., 2012; Schelhaas et al., 2003), potentially reducing the capability of forests to sustain carbon stocks (Galik and Jackson, 2009) and altering the biodiversity by changing the community composition (Chapin et al., 2000; Lavorel and Garnier, 2002).

Extensive analysis of the interactions between multiple disturbances has been generally focused on natural disturbances such as wildfire and insect outbreaks (Bebi et al., 2003; Bigler et al., 2005; Kulakowski and Veblen, 2002). However, similar analysis with anthropogenic disturbances such as forest harvest have been found to be challenging to conduct due to a lack of consistency and quality as well as the spatial and temporal extent of spatial records of historical harvest activity (White et al., 2017). Landsat time series provides synoptic and consistent data for mapping multiple disturbance types, enabling the study of interactions between natural and anthropogenic disturbances. The production of remotely-sensed spatially explicit datasets such as those

**Table 1**
Summary of multiple disturbances in Canadas's forested ecosystems (1985–2015), by total area, percentage of net ecosystem area and percentage of total disturbed area.

| | Disturbance type | Area [ha] | % of Canada's net forested ecosystem area | % of Canada's total disturbed area (1985–2015) |
|---|---|---|---|---|
| **No disturbance** | **Total** | **436,704,546** | **81.73** | - |
| **Disturbance (Greatest change 1985-2015)** | **Total** | **97,606,107** | **18.27** | **100** |
| | Fire | 49,851,292 | 9.33 | 51.07 |
| | Harvest | 19,688,088 | 3.68 | 20.17 |
| | Non-stand replacing | 28,066,727 | 5.25 | 28.76 |
| **1 disturbance** | **Total** | **84,094,643** | **15.74** | **86.16** |
| | Fire | 43,899,416 | 8.22 | 52.20 |
| | Harvest | 17,027,640 | 3.19 | 20.25 |
| | Non-stand replacing | 23,167,587 | 4.34 | 27.55 |
| **2 disturbances** | **Total** | **12,720,236** | **2.38** | **13.03** |
| | Fire-Fire | 1,393,876 | 0.26 | 1.43 |
| | Fire-Harvest | 142,025 | 0.03 | 0.15 |
| | Fire-NSR | 858,219 | 0.16 | 0.88 |
| | Harvest-Fire | 286,452 | 0.05 | 0.29 |
| | Harvest-Harvest | 1,081,279 | 0.20 | 1.11 |
| | Harvest-NSR | 442,820 | 0.08 | 0.45 |
| | NSR-Fire | 3,350,370 | 0.63 | 3.43 |
| | NSR-Harvest | 894,987 | 0.17 | 0.92 |
| | NSR-NSR | 4,270,208 | 0.80 | 4.37 |
| **≥3 disturbances** | **Total** | **791,229** | **0.15** | **0.81** |
| | Fire (as terminal disturbance) | 230,985 | 0.04 | 0.24 |
| | Harvest (as terminal disturbance) | 114,510 | 0.02 | 0.12 |
| | NSR (as terminal disturbance) | 445,734 | 0.08 | 0.46 |

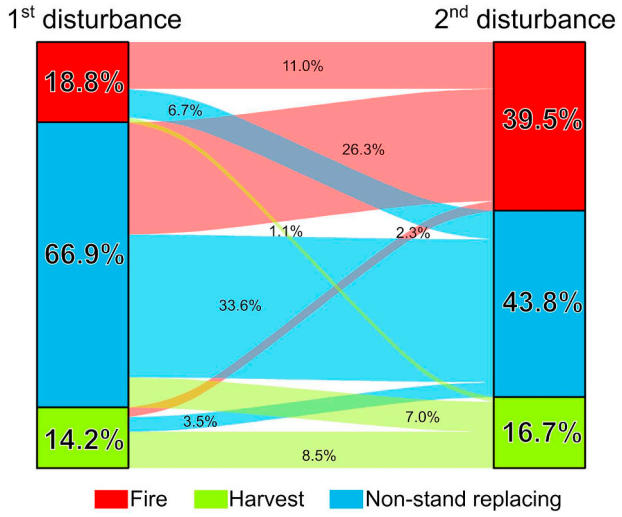


**Fig. 4.** Sankey diagram with the relationship between first (left) and second (right) disturbance event based on the change type. This graph represents the 2.38% of Canada's forested ecosystems that was impacted by two disturbances (1985–2015).

used herein is key to support modeling of multiple disturbances, as well as subsequent ecological processes, which in turn enables estimation of the probability of future disturbances (Bebi et al., 2003).

During the analyzed period (1985–2015), 18.27% of Canada's forested ecosystem area (discounting waterbodies) had some form of disturbance. Within this disturbed area, approximately 13.03% underwent two and 0.18% had three or more disturbances. Although fire is the main stand-replacing disturbance agent by area in Canada's forested ecosystems (Boulanger et al., 2012; Stocks et al., 2002), non-stand replacing disturbances prevailed in those instances where there were multiple disturbances (77% of multiple disturbance area). Moreover, a third of the total multiple disturbance area was caused by two consecutive non-stand replacing events. By definition, non-stand replacing disturbances do not involve broad vegetation removal, but a change in the vegetation condition, and hence they will result in more trees or other vegetation present to be subject to a second change relative to the stand replacing disturbances of wildfire and harvesting. Further, many of the multiple non-stand replacing disturbances are associated with areas dominated by wetlands (e.g., Hudson Plains ecozone, Fig. 3C; Wulder et al., 2018), where vegetation changes may be linked to variability in hydrological regimes and precipitation (e.g., vegetation stress, desiccation processes).

Wildfires following non-stand replacing disturbances involved approximately 26% of the multiple disturbance areas, and non-stand replacing disturbances followed by harvest events were approximately 7.2%. Long-term declining trends can indicate mature vegetation displaying a slow reduction in the spectral values, but also a variety of disturbance agents including pests, drought, and insect infestations. First non-stand replacing disturbances may prompt the immediate occurrence of subsequent stand replacing disturbances due to both natural (e.g., wildfire) or anthropogenic (e.g., preventive harvest, prescribed fires) factors. Fig. 2B shows an example for a declining spectral trend occurring over a long time period that is abruptly overridden by a stand-replacing disturbance. These multiple disturbances interactions are shown in Fig. 3A in the vicinity of Williams Lake, British Columbia, where preventative harvesting campaigns were executed as a strategy to reduce the impact and spread of a mountain pine beetle (*Dendroctonus ponderosae*) outbreak in the Montane Cordillera (Wulder et al., 2009). In this sense, the detection of non-stand replacing disturbances immediately followed by stand replacing (i.e., fire and harvest) can be defined as *linked*, with the first disturbance having legacy effect on the occurrence of the of second disturbance (Edwards et al., 2015; Johnstone et al., 2016). Non-stand replacing disturbances following fires are found across several years following the first event, reflecting delayed post-fire mortality of the residual vegetation (Bolton et al., 2015). Conversely, non-stand replacing disturbances occur

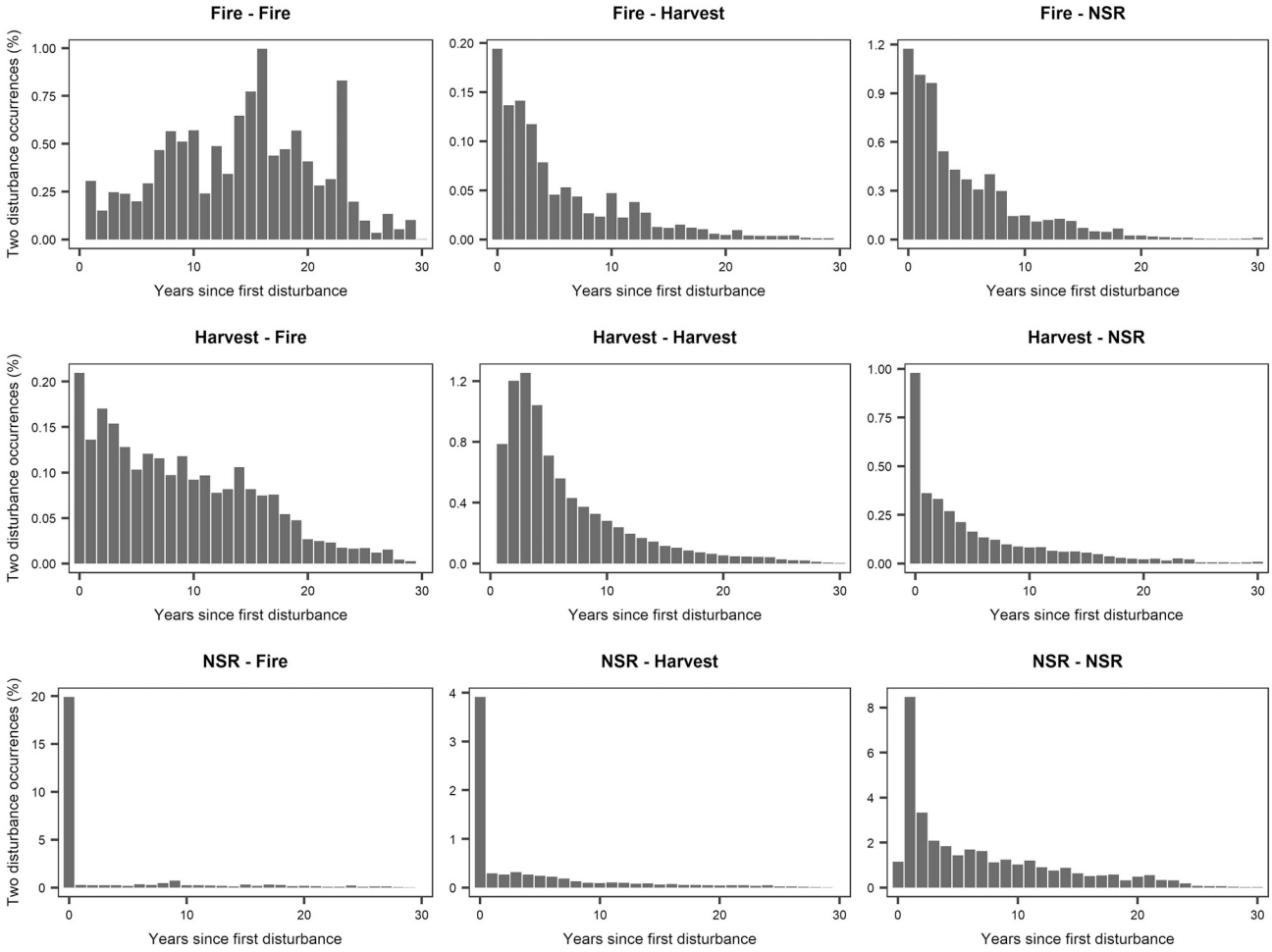


**Fig. 5.** Histograms of years between first and second change for each pair of change type combination. NSR: non-stand replacing disturbances. Note that y-axis range is different for each histogram.

immediately after the harvest events. Harvest disturbances are not always discrete events and after clearcutting sites can be prepared for planting and stand tending with soil scarification and herbicide treatment (Pidgen and Mallik, 2013).

Harvest-harvest interactions represented 8.5% of the multiple disturbance area and are likely related to harvesting practices (e.g., partial cutting), site preparation activities (e.g., mechanical, chemical), and silvicultural treatments (e.g., thinning) (Jarron et al., 2017; Thomas et al., 2011). Two consecutive wildfires involved 11% of the area that had two disturbances during the analysis period. The fire-fire interaction had a scattered distribution of time since previous disturbance values (Fig. 5), which is related to the arbitrary nature of fires, typically ignited by lightning strike, that can occur widely across boreal forested ecosystems as opposed to human related activities (e.g., harvest) which are confined within managed areas. Natural disturbances rarely eliminate all structural elements from the disturbed site (Franklin et al., 2002), which combined with the high productivity of some forested ecosystems in Canada allows for accumulating fuel that can be burned by a second wildfire within the 30 year period analyzed. This situation is shown in Fig. 3B, focusing upon a fire-dominated area within the Boreal Shield West ecozone, which has one of the shortest fire return intervals (Coops et al., 2018; Stocks et al., 2002), and hence is more prone to the occurrence of short-interval fire disturbances.

Fire-harvest and harvest-fire interactions occur with the least frequency (Fig. 4). This is seen as a result of wildfires and harvest activities generally occurring in different geographical areas: harvesting is commonly present in more southern latitudes in conjunction with forest management practices where wildfire events are uncommon due to fire suppression (White et al., 2017). An example of these multiple disturbance interactions between wildfire and harvest is displayed in Fig. 3D, which shows a 1991 wildfire that affected a heavily managed forested area close in the vicinity of Betsiamites River, Quebec (Environment Canada, 1991). In addition, fire-harvest and harvest-fire interactions also relate several forest management practices such as salvage cutting activities of damaged trees following wildfires (Thomas et al., 2011), and clearcutting followed by prescribed burning of the remaining vegetation (slash and burn) (Beaudry et al., 2011).

Using the spectral information provided by the annual time series of seamless surface reflectance composites representing temporally-fitted spectral values, we spectrally characterized disturbances (via change rate, Fig. 6) and post-disturbance vegetation regrowth (via recovery indicator, Fig. 7). Overall, fires had the highest variability in spectral change rate, which is expected as wildfires occur over a broader range of forest conditions and land cover types in comparison to harvest activities which typically take place in productive forest areas with greater pre-disturbance forest cover (White et al., 2017). Wildfires involved in multiple disturbances had change rates analogous to those instances with a single wildfire. The recovery indicator, however, indicates a more rapid short-term vegetation regrowth from fires that burned previously harvested areas (24% higher), which could suggest the establishment of vegetation communities different to areas with a single harvest event (Pidgen and Mallik, 2013). The results here presented would suggest that harvest-fire interactions are *compounded* as the rate of recovery to a similar spectral state from the previous

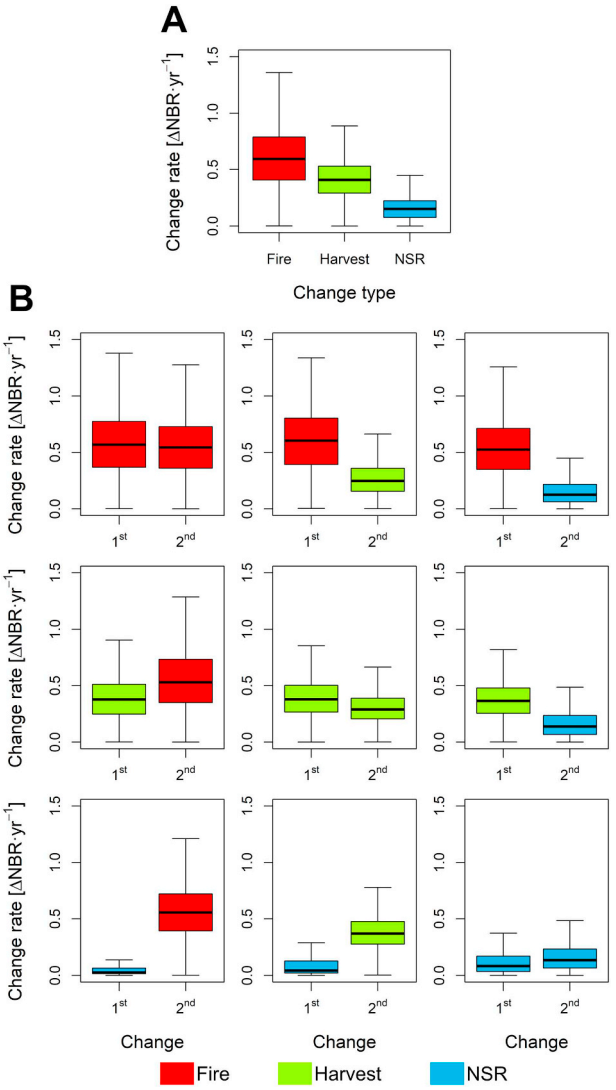


**Fig. 6.** Boxplots representing median, interquartile range, and extreme values of change rate metric ($\Delta NBR \cdot yr^{-1}$). (A) Reference value distribution per change type for pixels with only one disturbance. (B) Value distribution for first and second disturbance for each change type combination. NSR: non-stand replacing disturbances.

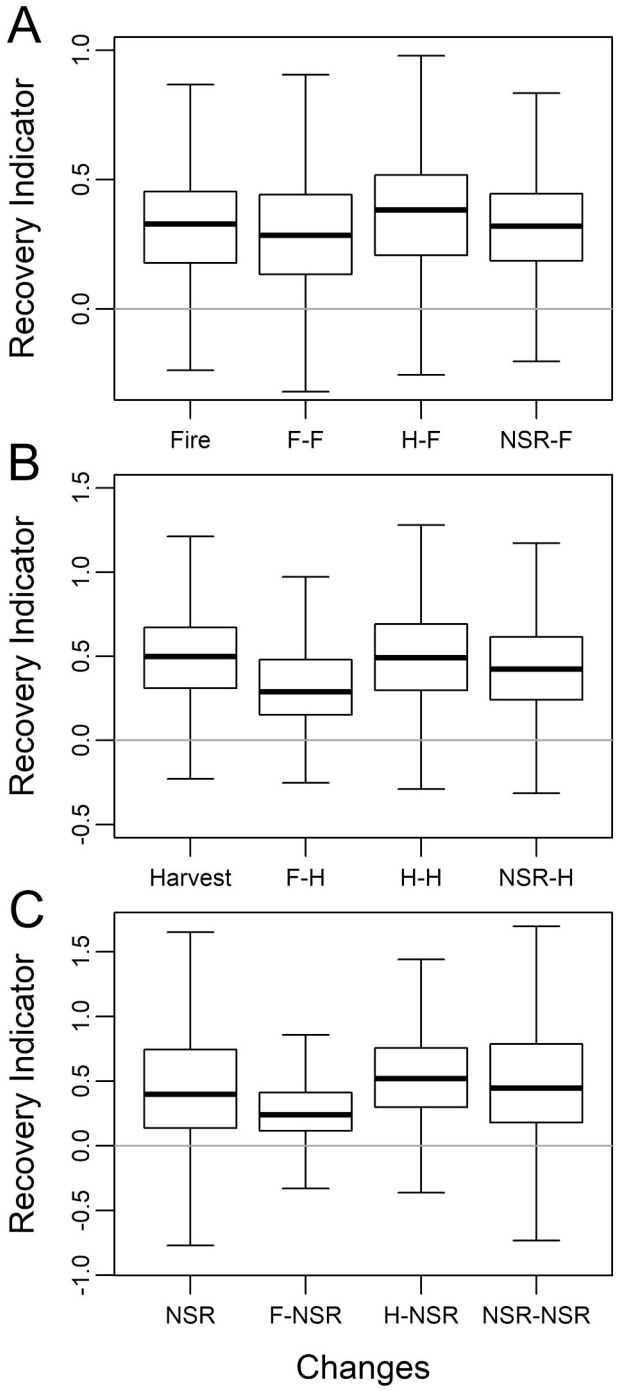


**Fig. 7.** Boxplots representing median, interquartile range, and extreme values of recovery indicator after (A) fire, (B) harvest, and (C) non-stand replacing disturbances. Left boxes represent values for single disturbances (as reference), and the remainder represent the recovery indicator following the second disturbance different combination of multiple disturbances for fire (F), harvest (H), and non-stand replacing (NSR) disturbances.

disturbance has been altered (Buma, 2015). Short-term recovery of fire-harvest interactions was on average 39% lower than locations with single harvest events, likely influenced in part by differences in site productivity. Notably, the median recovery indicator for fire-harvest interactions (0.34) is comparable to the median recovery indicator value resulting from single fire events (0.33). Areas that were disturbed by two harvest events resulted in the highest recovery indicator values (median = 0.62) and a 10% increase compared to single harvest events, which denotes the higher productivity of the forested ecosystems where these practices take place (Masek et al., 2011).

The distribution of change rate values for non-stand replacing disturbances followed by wildfires is lower and less scattered than when non-stand replacing disturbance preceding harvest activities. This might indicate fires occur on mature vegetation which exhibits in the time-series a long-term reduction in the spectral response, while these harvest events were likely triggered by preventive management responses to pest or diseases outbreaks. In both cases, the regrowth of vegetation was found to be comparable to single disturbance wildfires and harvest, respectively. Short-term vegetation recovery for non-stand replacing disturbances following harvest events and following non-stand replacing disturbances is comparable to instances with a single non-stand replacing event. However, the recovery indicator results suggest a slower vegetation regrowth for non-stand replacing disturbances following wildfires to the status previous to the second disturbance event.

The results presented demonstrate the prevalence of non-stand replacing disturbances in the occurrence of multiple disturbances. Given the lower magnitude of change and the typical lack of association of non-stand replacing disturbances with a change in the land cover class,

non-stand replacing changes are not typically systematically mapped and reported (Ahmed et al., 2017; Bell et al., 2018; Cohen et al., 2016; Franklin et al., 2015). Forest change information derived from Landsat data using the C2C approach provided the ability to analyze multiple disturbances involving non-stand replacing changes. More detailed categorization of non-stand replacing disturbances (e.g., insect disturbances, pests, water stress) would be desirable and would enrich the analysis and our understanding of the interactions between multiple disturbances. However, given the diverse nature of the non-stand replacing disturbances and their various manifestations (e.g., mortality, defoliation) depending on the disturbance agent and nature of the vegetation affected, it is challenging to further break down non-stand replacing disturbances in more detailed subcategories exclusively using multi-spectral data (Senf et al., 2017).

Future research on multiple disturbances will offer unique opportunities for investigation due to increasingly longer records of Earth observation data. The Landsat program has acquired geo-radiometically calibrated, 30-m data since 1982, with more frequent acquisition starting in 1984 with the launch of Landsat-5 TM. As a result, Landsat's archive is a unique window into the past, providing an invaluable, free and open data source, to monitor forest dynamics and other global phenomena (Wulder et al., 2012). Currently Landsat-8 OLI and Sentinel-2 are acquiring hundreds of observations daily, the launch of Landsat-9 is scheduled for December 2020, and Landsat-10 planning is ongoing (Wulder et al., 2019). In addition to future acquisitions, novel methods for developing and standardizing Landsat MSS products for inclusion in time series analyses are acting to reliably extend the monitoring period to start in 1972 (Savage et al., 2018; Vogeler et al., 2018).

## 6. Conclusions

In this research, we used annual forest change information derived from a three-decade time series of Landsat imagery to capture and perform an assessment of the multiple disturbances found over 650 Mha of Canada's forested ecosystems from 1985 to 2015. Frequency, distribution, and causes of multiple forest disturbances, and subsequent vegetation recovery were analyzed using the disturbance agent attribution (fire, harvest, and non-stand replacing disturbances) and spectral metrics derived from the time series of Landsat imagery characterizing change (change rate and time between disturbances) and following vegetation regrowth (recovery indicator). The results indicated that for the analyzed period, 18.27% of Canada's forested ecosystems (excluding waterbodies) underwent disturbances, and 2.53% was impacted by multiple disturbances (two or more disturbance events). Moreover, and although wildfires are the principal stand replacing disturbance agent by area in Canada's forests, the majority of multiple disturbances involved non-stand replacing events. Most of multiple disturbances presented a similar behaviour to single disturbance events in terms of spectral disturbance characterization. Lower spectral recovery rates were found on harvest and non-stand replacing events following wildfires, and higher recovery rates after fires subsequent to harvest activity. Outcomes of this research provide insights regarding the interaction between multiple disturbances and can in turn inform subsequent stand establishment and longer-term growth expectations. This information is valuable to advise planning activities for sustainable forest management and to inform expectations of future carbon stocks and models of greenhouse gas exchanges with the atmosphere.

## Acknowledgments

This research was undertaken as part of the “Earth Observation to Inform Canada's Climate Change Agenda (EO3C)” project jointly funded by the Canadian Space Agency (CSA), Government Related Initiatives Program (GRIP), and the Canadian Forest Service (CFS) of Natural Resources Canada (NRCan). Geordie Hobart, of the Canadian Forest Service, is thanked for his assistance in acquiring the Landsat data and preparing the annual best-available pixel image composites. This research was enabled in part by the computational support provided by WestGrid (www.westgrid.ca) and Compute Canada (www.computecanada.ca).

## References

Ahmed, O.S., Wulder, M.A., White, J.C., Hermosilla, T., Coops, N.C., Franklin, S.E., 2017. Classification of annual non-stand replacing boreal forest change in Canada using Landsat time series: a case study in northern Ontario. Remote Sens. Lett. 8, 29–37. https://doi.org/10.1080/2150704X.2016.1233371.

Banskota, A., Kayastha, N., Falkowski, M.J., Wulder, M.A., Froese, R.E., White, J.C., 2014. Forest monitoring using Landsat time series data: a review. Can. J. Remote. Sens. 40, 362–384. https://doi.org/10.1080/07038992.2014.987376.

Beaudry, S., Duchesne, L.C., CôTé, B., 2011. Short-term effects of three forestry practices on carabid assemblages in a jack pine forest. Can. J. For. Res. 27, 2065–2071. https://doi.org/10.1139/x97-171.

Bebi, P., Kulakowski, D., Veblen, T.T., 2003. Interactions between fire and spruce beetles in a subalpine rocky mountain forest landscape. Ecology 84, 362–371.

Beisner, B.E., Haydon, D.T., Cuddington, K.C., 2003. Alternative stable states in ecology. Alternative stable states in ecology. Front. Ecol. Environ. 1, 376–382. https://doi.org/10.2307/3868190.

Bell, D.M., Cohen, W.B., Reilly, M., Yang, Z., 2018. Visual interpretation and time series modeling of Landsat imagery highlight drought's role in forest canopy declines. Ecosphere 9. https://doi.org/10.1002/ecs2.2195.

Bigler, C., Kulakowski, D., Veblen, T.T., 2005. Multiple disturbance interactions and drought influence fire severity in rocky mountain subalpine forests. Ecology 86, 3018–3029. https://doi.org/10.1890/05-0011.

Bolton, D.K., Coops, N.C., Wulder, M.A., 2015. Characterizing residual structure and forest recovery following high-severity fire in the western boreal of Canada using Landsat time-series and airborne lidar data. Remote Sens. Environ. 163, 48–60. https://doi.org/10.1016/j.rse.2015.03.004.

Boulanger, Y., Gauthier, S., Burton, P.J., Vaillancourt, M.A., 2012. An alternative fire regime zonation for Canada. Int. J. Wildl. Fire 21, 1052–1064. https://doi.org/10.1071/WF11073.

Bradford, J.B., Fraver, S., Milo, A.M., D'Amato, A.W., Palik, B., Shinneman, D.J., 2012. Effects of multiple interacting disturbances and salvage logging on forest carbon stocks. For. Ecol. Manag. 267, 209–214. https://doi.org/10.1016/j.foreco.2011.12.010.

Buma, B., 2015. Disturbance interactions: characterization, prediction, and the potential for cascading effects. Ecosphere 6, 1–15. https://doi.org/10.1890/ES15-00058.1.

Buma, B., Wessman, C.A., 2011. Disturbance interactions can impact resilience mechanisms of forests. Ecosphere 2, 1–13. https://doi.org/10.1890/ES11-00038.1.

Chapin, F.S., Zavaleta, E.S., Eviner, V.T., Naylor, R.L., Vitousek, P.M., Reynolds, H.L., Hooper, D.U., Lavorel, S., Sala, O.E., Hobbie, S.E., Mack, M.C., Diaz, S., 2000. Consequences of changing biodiversity. Nature 405, 234–242.

Cobb, T.P., Langor, D.W., Spence, J.R., 2007. Biodiversity and multiple disturbances: boreal forest ground beetle (Coleoptera: Carabidae) responses to wildfire, harvesting, and herbicide. Can. J. For. Res. 37, 1310–1323. https://doi.org/10.1139/x06-310.

Cohen, W.B., Goward, S.N., 2004. Landsat's role in ecological applications of remote sensing. Bioscience 54, 535. https://doi.org/10.1641/0006-3568(2004)054[0535:LRIEAO]2.0.CO;2.

Cohen, W.B., Yang, Z., Stehman, S.V., Schroeder, T.A., Bell, D.M., Masek, J.G., Huang, C., Meigs, G.W., 2016. Forest disturbance across the conterminous United States from 1985 to 2012: the emerging dominance of forest decline. For. Ecol. Manag. 360, 242–252. https://doi.org/10.1016/j.foreco.2015.10.042.

Cohen, W.B., Yang, Z., Healey, S.P., Kennedy, R.E., Gorelick, N., 2018. A LandTrendr multispectral ensemble for forest disturbance detection. Remote Sens. Environ. 205, 131–140. https://doi.org/10.1016/j.rse.2017.11.015.

Coops, N.C., Hermosilla, T., Wulder, M.A., White, J.C., Bolton, D.K., 2018. A thirty year, fine-scale, characterization of area burned in Canadian forests shows evidence of regionally increasing trends in the last decade. PLoS One 13, e0197218. https://doi.org/10.1371/journal.pone.0197218.

Cuba, N., 2015. Research note: Sankey diagrams for visualizing land cover dynamics. Landsc. Urban Plan. 139, 163–167. https://doi.org/10.1016/j.landurbplan.2015.03.010.

Edwards, M., Krawchuk, M.A., Burton, P.J., 2015. Short-interval disturbance in lodgepole pine forests, British Columbia, Canada: understory and overstory response to mountain pine beetle and fire. For. Ecol. Manag. 338, 163–175. https://doi.org/10.1016/j.foreco.2014.11.011.

Environment Canada, 1991. Severe forest fire outbreak in Quebec. Clim. Perspect. 13, 1.

Franklin, J.F., Shaw, D.C., Bible, K., Chen, J., Spies, T.A., Pelt, R. Van, Carey, A.B., Thornburgh, D.A., Berg, D.R., Lindenmayer, D.B., Harmon, M.E., Keeton, W.S., 2002. Disturbances and structural development of natural forest ecosystems with silvicultural implications, using Douglas-fir forests as an example. For. Ecol. Manag. 155, 399–423. https://doi.org/10.1016/S0378-1127(01)00575-8.

Franklin, S.E., Ahmed, O.S., Wulder, M.A., White, J.C., Hermosilla, T., Coops, N.C., 2015. Large area mapping of annual land cover dynamics using multi-temporal change detection and classification of Landsat time series data. Can. J. Remote. Sens. 41, 293–314. https://doi.org/10.1080/07038992.2015.1089401.

Frazier, R.J., Coops, N.C., Wulder, M.A., 2015. Boreal shield forest disturbance and

recovery trends using Landsat time series. Remote Sens. Environ. 170, 317–327. https://doi.org/10.1016/j.rse.2015.09.015.
Galik, C.S., Jackson, R.B., 2009. Risks to forest carbon offset projects in a changing climate. For. Ecol. Manag. 257, 2209–2216. https://doi.org/10.1016/j.foreco.2009.03.017.
Gillis, M.D., Leckie, D.G., 1996. Forest inventory update in Canada. For. Chron. 72, 138–156. https://doi.org/10.5558/tfc72138-2.
Goward, S.N., Masek, J.G., Cohen, W.B., Moisen, G.G., Collatz, G.J., Healey, S.P., Houghton, R.A., Huang, C., Kennedy, R.E., Law, B., Powell, S.L., Turner, D., Wulder, M.A., 2008. Forest disturbance and north American carbon flux. Eos (Washington. DC) 89, 28–30.
Griffiths, P., Linden, S. Van Der, Kuemmerle, T., Hostert, P., 2013. A pixel-based Landsat compositing algorithm for large area land cover mapping. IEEE J. Sel. Top. Appl. Earth Obs. Remote Sens. 6, 2088–2101.
Hermosilla, T., Wulder, M.A., White, J.C., Coops, N.C., Hobart, G.W., 2015a. An integrated Landsat time series protocol for change detection and generation of annual gap-free surface reflectance composites. Remote Sens. Environ. 158, 220–234. https://doi.org/10.1016/j.rse.2014.11.005.
Hermosilla, T., Wulder, M.A., White, J.C., Coops, N.C., Hobart, G.W., 2015b. Regional detection, characterization, and attribution of annual forest change from 1984 to 2012 using Landsat-derived time-series metrics. Remote Sens. Environ. 170, 121–132. https://doi.org/10.1016/j.rse.2015.09.004.
Hermosilla, T., Wulder, M.A., White, J.C., Coops, N.C., Hobart, G.W., Campbell, L.B., 2016. Mass data processing of time series Landsat imagery: pixels to data products for forest monitoring. Int. J. Digit. Earth 9, 1035–1054. https://doi.org/10.1080/17538947.2016.1187673.
Hermosilla, T., Wulder, M.A., White, J.C., Coops, N.C., Hobart, G.W., 2017. Updating Landsat time series of surface-reflectance composites and forest change products with new observations. Int. J. Appl. Earth Obs. Geoinf. 63, 104–111. https://doi.org/10.1016/j.jag.2017.07.013.
Hermosilla, T., Wulder, M.A., White, J.C., Coops, N.C., Hobart, G.W., 2018. Disturbance-informed annual land cover classification maps of Canada's forested ecosystems for a 29-year Landsat time series. Can. J. Remote. Sens. 44, 67–87. https://doi.org/10.1080/07038992.2018.1437719.
Hirsch, A.I., Little, W.S., Houghton, R.A., Scott, N.A., White, J.D., 2004. The net carbon flux due to deforestation and forest re-growth in the Brazilian Amazon: analysis using a process-based model. Glob. Chang. Biol. 10, 908–924. https://doi.org/10.1111/j.1529-8817.2003.00765.x.
Horler, D.N., Ahern, F.J., 1986. Forestry information content of thematic mapper data. Int. J. Remote Sens. https://doi.org/10.1080/01431168608954695.
Huang, C., Goward, S.N., Masek, J.G., Thomas, N., Zhu, Z., Vogelmann, J.E., 2010. An automated approach for reconstructing recent forest disturbance history using dense Landsat time series stacks. Remote Sens. Environ. 114, 183–198. https://doi.org/10.1016/j.rse.2009.08.017.
Jarron, L.R., Hermosilla, T., Coops, N.C., Wulder, M.A., White, J.C., Hobart, G.W., Leckie, D.G., 2017. Differentiation of alternate harvesting practices using annual time series of landsat data. Forests 8. https://doi.org/10.3390/f8010015.
Johnstone, J.F., Allen, C.D., Franklin, J.F., Frelich, L.E., Harvey, B.J., Higuera, P.E., Mack, M.C., Meentemeyer, R.K., Metz, M.R., Perry, G.L.W., Schoennagel, T., Turner, M.G., 2016. Changing disturbance regimes, ecological memory, and forest resilience. Front. Ecol. Environ. 14, 369–378. https://doi.org/10.1002/fee.1311.
Kangas, A., Maltamo, M., 2006. Forest Inventory. Methodology and Applications. Springer.
Kennedy, R.E., Yang, Z., Cohen, W.B., 2010. Detecting trends in forest disturbance and recovery using yearly Landsat time series: 1. LandTrendr — temporal segmentation algorithms. Remote Sens. Environ. 114, 2897–2910. https://doi.org/10.1016/j.rse.2010.07.008.
Kennedy, R.E., Yang, Z., Cohen, W.B., Pfaff, E., Braaten, J., Nelson, P., 2012. Spatial and temporal patterns of forest disturbance and regrowth within the area of the Northwest Forest Plan. Remote Sens. Environ. 122, 117–133. https://doi.org/10.1016/j.rse.2011.09.024.
Kennedy, R.E., Andréfouët, S., Cohen, W.B., Gómez, C., Griffiths, P., Hais, M., Healey, S.P., Helmer, E.H., Hostert, P., Lyons, M.B., Meigs, G.W., Pflugmacher, D., Phinn, S.R., Powell, S.L., Scarth, P., Sen, S., Schroeder, T.A., Schneider, A., Sonnenschein, R., Vogelmann, J.E., Wulder, M.A., Zhu, Z., 2014. Bringing an ecological view of change to landsat-based remote sensing. Front. Ecol. Environ. 12, 339–346. https://doi.org/10.1890/130066.
Kennedy, R.E., Ohmann, J., Gregory, M., Roberts, H., Yang, Z., Bell, D.M., Kane, V., Hughes, M.J., Cohen, W.B., Powell, S., Neeti, N., Larrue, T., Hooper, S., Kane, J., Miller, D.L., Perkins, J., Braaten, J., Seidl, R., 2018. An empirical, integrated forest biomass monitoring system. Environ. Res. Lett. 13. https://doi.org/10.1088/1748-9326/aa9d9e.
Keogh, E., Chu, S., Hart, D., Pazzani, M., 2001. An online algorithm for segmenting time series. In: Data Mining, 2001. ICDM, Proceedings IEEE International Conference on. IEEE Comput. Soc, San Jose, CA, pp. 289–296. https://doi.org/10.1109/ICDM.2001.989531.
Key, C.H., Benson, N.C., 2006. Landscape assessment: Sampling and analysis methods. In: USDA For. Serv. Gen. Tech. Rep. RMRS-GTR-164-CD, pp. 1–55.
Kulakowski, D., Veblen, T.T., 2002. Influences of fire history and topography on the pattern of a severe wind blowdown in a Colorado subalpine forest. J. Ecol. 90, 806–819. https://doi.org/10.1046/j.1365-2745.2002.00722.x.
Kurz, W.A., Dymond, C.C., Stinson, G., Rampley, G.J., Neilson, E.T., Carroll, A.L., Ebata, T., Safranyik, L., 2008. Mountain pine beetle and forest carbon feedback to climate change. Nature 452, 987–990. https://doi.org/10.1038/nature06777.
Kurz, W.A., Dymond, C.C., White, T., Stinson, G., Shaw, C.H., Rampley, G.J., Smyth, C., Simpson, B.N., Neilson, E.T., Trofymow, J.A., Metsaranta, J., Apps, M.J., 2009. CBM-CFS3: a model of carbon-dynamics in forestry and land-use change implementing IPCC standards. Ecol. Model. 220, 480–504. https://doi.org/10.1016/j.ecolmodel.2008.10.018.
Lavoie, L., Sirois, L., 1998. Vegetation changes caused by recent fires in the northern boreal forest of eastern Canada. J. Veg. Sci. 9, 483–492.
Lavorel, S., Garnier, E., 2002. Predicting changes in community composition and ecosystem functioning from plant traits: revisiting the holy grail. Funct. Ecol. 16, 545–556.
Masek, J.G., Vermote, E.F., Saleous, N.E., Wolfe, R., Hall, F.G., Huemmrich, K.F., Gao, F., Kutler, J., Lim, T.K., 2006. A Landsat surface reflectance dataset for North America, 1990-2000. In: Geosci. Remote Sens. Lett. vol. 3. IEEE, pp. 68–72.
Masek, J.G., Cohen, W.B., Leckie, D., Wulder, M.A., Vargas, R., de Jong, B., Healey, S., Law, B., Birdsey, R., Houghton, R.a., Mildrexler, D., Goward, S., Smith, W.B., 2011. Recent rates of forest harvest and conversion in North America. J. Geophys. Res. 116, 1–22. https://doi.org/10.1029/2010JG001471.
Maynard, D.G., Paré, D., Thiffault, E., Lafleur, B., Hogg, K.E., Kishchuk, B., 2014. How do natural disturbances and human activities affect soils and tree nutrition and growth in the Canadian boreal forest? Environ. Rev. 22, 161–178. https://doi.org/10.1139/er-2013-0057.
Oliver, C.D., Larson, B.C., 1990. Forest Stand Dynamics. John Wiley and Sons, New York, NY.
Olofsson, P., Foody, G.M., Herold, M., Stehman, S.V., Woodcock, C.E., Wulder, M.A., 2014. Good practices for estimating area and assessing accuracy of land change. Remote Sens. Environ. 148, 42–57. https://doi.org/10.1016/j.rse.2014.02.015.
Pickell, P.D., Hermosilla, T., J. Frazier R, Coops, N.C., Wulder, M.A., 2016. Forest recovery trends derived from Landsat time series for north American boreal forests. Int. J. Remote Sens. 37, 138–149. doi:https://doi.org/10.1080/2150704X.2015.1126375.
Pidgen, K., Mallik, A.U., 2013. Ecology of compounding disturbances: the effects of prescribed burning after clearcutting. Ecosystems 16, 170–181. https://doi.org/10.1007/s10021-012-9607-2.
Price, D.T., Alfaro, R.I., Brown, K.J., Flannigan, M.D., Fleming, R. a, Hogg, E.H., Girardin, M.P., Lakusta, T., Johnston, M., Mckenney, D.W., Pedlar, J.H., Stratton, T., Sturrock, R.N., Thompson, I.D., Trofymow, J. a, Venier, L. a, 2013. Anticipating the consequences of climate change for Canada's boreal forest ecosystems 1. Environ. Rev. 21, 322–365.
Roy, D.P., Ju, J., Kline, K., Scaramuzza, P.L., Kovalskyy, V., Hansen, M., Loveland, T.R., Vermote, E., Zhang, C., 2010. Web-enabled Landsat data (WELD): Landsat ETM+ composited mosaics of the conterminous United States. Remote Sens. Environ. 114, 35–49. https://doi.org/10.1016/j.rse.2009.08.011.
Savage, S.L., Lawrence, R.L., Squires, J.R., Holbrook, J.D., Olson, L.E., Braaten, J.D., Cohen, W.B., 2018. Shifts in forest structure in Northwest Montana from 1972 to 2015 using the landsat archive from multispectral scanner to operational land imager. Forests 9, 1–20. https://doi.org/10.3390/f9040157.
Schelhaas, M.J., Nabuurs, G.J., Schuck, A., 2003. Natural disturbances in the European forests in the 19th and 20th centuries. Glob. Chang. Biol. 9, 1620–1633. https://doi.org/10.1046/j.1529-8817.2003.00684.x.
Schmidt, G.L., Jenkerson, C.B., Masek, J., Vermote, E., Gao, F., 2013. Landsat Ecosystem Disturbance Adaptive Processing System (LEDAPS) Algorithm Description.
Schmidt, M., 2008. The Sankey diagram in energy and material flow management: part I: history. J. Ind. Ecol. 12, 82–94. https://doi.org/10.1111/j.1530-9290.2008.00004.x.
Senf, C., Seidl, R., Hostert, P., 2017. Remote sensing of forest insect disturbances: current state and future directions. Int. J. Appl. Earth Obs. Geoinf. 60, 49–60. https://doi.org/10.1016/j.jag.2017.04.004.
Stewart, B.P., Wulder, M.A., McDermid, G.J., Nelson, T.A., 2009. Disturbance capture and attribution through the integration of Landsat and IRS-1C imagery. Can. J. Remote. Sens. 35, 523–533.
Stocks, B.J., Mason, J.A., Todd, J.B., Bosch, E.M., Wotton, B.M., Amiro, B.D., Flannigan, M.D., Hirsch, K.G., Logan, K.A., Martell, D.L., Skinner, W.R., 2002. Large forest fires in Canada, 1959–1997. J. Geophys. Res. 108. https://doi.org/10.1029/2001JD000484.
Thomas, N.E., Huang, C., Goward, S.N., Powell, S., Rishmawi, K., Schleeweis, K., Hinds, A., 2011. Validation of North American Forest disturbance dynamics derived from Landsat time series stacks. Remote Sens. Environ. 115, 19–32. https://doi.org/10.1016/j.rse.2010.07.009.
Turner, M.G., Braziunas, K.H., Hansen, W.D., Harvey, B.J., 2019. Short-interval severe fire erodes the resilience of subalpine lodgepole pine forests. Proc. Natl. Acad. Sci. 116, 201902841. https://doi.org/10.1073/pnas.1902841116.
Vepakomma, U., Kneeshaw, D., St-Onge, B., 2010. Interactions of multiple disturbances in shaping boreal forest dynamics: a spatially explicit analysis using multi-temporal lidar data and high-resolution imagery. J. Ecol. 98, 526–539. https://doi.org/10.1111/j.1365-2745.2010.01643.x.
Verbesselt, J., Hyndman, R., Zeileis, A., Culvenor, D.S., Newnham, G.J., 2010. Detecting trend and seasonal changes in satellite image time series. Remote Sens. Environ. 114, 106–115. https://doi.org/10.1016/j.rse.2010.08.003.
Vogeler, J.C., Braaten, J.D., Slesak, R.A., Falkowski, M.J., 2018. Extracting the full value of the Landsat archive: inter-sensor harmonization for the mapping of Minnesota forest canopy cover (1973–2015). Remote Sens. Environ. 209, 363–374. https://doi.org/10.1016/j.rse.2018.02.046.
White, J.C., Wulder, M.A., 2014. The Landsat observation record of Canada: 1972–2012. Can. J. Remote. Sens. 39, 455–467.
White, J.C., Wulder, M.A., Hobart, G.W., Luther, J.E., Hermosilla, T., Griffiths, P., Coops, N.C., Hall, R.J., Hostert, P., Dyk, A., Guindon, L., 2014. Pixel-based image compositing for large-area dense time series applications and science. Can. J. Remote. Sens. 40, 192–212. https://doi.org/10.1080/07038992.2014.945827.
White, J.C., Wulder, M.A., Hermosilla, T., Coops, N.C., Hobart, G.W., 2017. A nationwide

annual characterization of 25 years of forest disturbance and recovery for Canada using Landsat time series. Remote Sens. Environ. 194, 303–321. https://doi.org/10.1016/j.rse.2017.03.035.

Wilson, B.T., Woodall, C.W., Griffith, D.M., 2013. Imputing forest carbon stock estimates from inventory plots to a nationally continuous coverage. Carbon Balance Manag 8, 1–15. https://doi.org/10.1186/1750-0680-8-1.

Woodcock, C.E., Allen, R., Anderson, M., Belward, A., Bindschadler, R., Cohen, W., Gao, F., Goward, S.N., Helder, D.L., Helmer, E.H., Nemani, R.R., Oreopoulos, L., Schott, J., Thenkabail, P.S., Vermonte, E., Vogelmann, J.E., Wulder, M.A., Wynne, R.H., 2008. Free access to Landsat imagery. Science (80-.) 320, 1011. https://doi.org/10.1126/science.320.5879.1011a.

Woods, A.J., Coates, K.D., Watts, M., Foord, V., Holtzman, E.I., 2017. Warning signals of adverse interactions between climate change and native stressors in British Columbia forests. Forests 8, 1–21. https://doi.org/10.3390/f8080280.

Wulder, M.A., Kurz, W.A., Gillis, M., 2004. National level forest monitoring and modeling in Canada. Prog. Plann. 61, 365–381.

Wulder, M.A., White, J.C., Cranny, M.M., Hall, R.J., Luther, J.E., Beaudoin, A., Goodenough, D.G., Dechka, J.A., 2008. Monitoring Canada's forests. Part 1: completion of the EOSD land cover project. Can. J. Remote. Sens. 34, 549–562.

Wulder, M.A., White, J.C., Grills, D., Nelson, T., Coops, N.C., 2009. Aerial overview survey of the mountain pine beetle epidemic in British Columbia: communication of impacts. BC J. Ecosyst. Manag. 10, 45–58.

Wulder, M.A., Masek, J.G., Cohen, W.B., Loveland, T.R., Woodcock, C.E., 2012. Opening the archive: how free data has enabled the science and monitoring promise of Landsat. Remote Sens. Environ. 122, 2–10. https://doi.org/10.1016/j.rse.2012.01.010.

Wulder, M.A., White, J.C., Loveland, T.R., Woodcock, C.E., Belward, A.S., Cohen, W.B., Fosnight, E.A., Shaw, J., Masek, J.G., Roy, D.P., 2016. The global Landsat archive: status, consolidation, and direction. Remote Sens. Environ. 185, 271–283. https://doi.org/10.1016/j.rse.2015.11.032.

Wulder, M.A., Li, Z., Campbell, E.M., White, J.C., Hobart, G., Hermosilla, T., Coops, N.C., 2018. A national assessment of wetland status and trends for Canada's forested ecosystems using 33 years of earth observation satellite data. Remote Sens. 10, 1623. https://doi.org/10.3390/rs10101623.

Wulder, M.A., Loveland, T.R., Roy, D.P., Crawford, C.J., Masek, J.G., Woodcock, C.E., Allen, R.G., Anderson, M.C., Belward, A.S., Cohen, W.B., Dwyer, J., Erb, A., Gao, F., Griffiths, P., Helder, D., Hermosilla, T., Hipple, J.D., Hostert, P., Hughes, M.J., Huntington, J., Johnson, D.M., Kennedy, R., Kilic, A., Li, Z., Lymburner, L., McCorkel, J., Pahlevan, N., Scambos, T.A., Schaaf, C., Schott, J.R., Sheng, Y., Storey, J., Vermote, E., Vogelmann, J., White, J.C., Wynne, R.H., Zhu, Z., 2019. Current status of Landsat program, science, and applications. Remote Sens. Environ. 225, 127–147. https://doi.org/10.1016/j.rse.2019.02.015.

Zhu, Z., 2017. Change detection using landsat time series: a review of frequencies, preprocessing, algorithms, and applications. ISPRS J. Photogramm. Remote Sens. 130, 370–384. https://doi.org/10.1016/j.isprsjprs.2017.06.013.

Zhu, Z., Woodcock, C.E., 2012. Object-based cloud and cloud shadow detection in Landsat imagery. Remote Sens. Environ. 118, 83–94. https://doi.org/10.1016/j.rse.2011.10.028.

Zhu, Z., Woodcock, C.E., 2014. Continuous change detection and classification of land cover using all available Landsat data. Remote Sens. Environ. 144, 152–171. https://doi.org/10.1016/j.rse.2014.01.011.

Zhu, Z., Wulder, M.A., Roy, D.P., Woodcock, C.E., Hansen, M.C., Radeloff, V.C., Healey, S.P., Schaaf, C., Hostert, P., Strobl, P., Pekel, J.F., Lymburner, L., Pahlevan, N., Scambos, T.A., 2019. Benefits of the free and open Landsat data policy. Remote Sens. Environ. 224, 382–385. https://doi.org/10.1016/j.rse.2019.02.016.